Pergamon

J. Phys. Chem. Solids Vol. 55, No. 5, pp. 391–404, 1994

0022-3697/94 $7.00 + 0.00

MODEL CALCULATIONS OF PHASE STABILITIES OF OXIDE SOLID SOLUTIONS IN THE Co–Fe–Mn–O SYSTEM AT 1200°C

RAMESH SUBRAMANIAN,† RÜDIGER DIECKMANN,† GUNNAR ERIKSSON‡ and ARTHUR PELTON‡

†Department of Materials Science and Engineering, Bard Hall, Cornell University, Ithaca, NY 14853-1501, U.S.A.

‡Centre de Recherche en Calcul Thermochemique, École Polytechnique, Montréal, Québec, Canada

(*Received* 28 *September* 1993; *accepted* 5 *January* 1994)

Abstract—The thermodynamics of the spinel and rock-salt structure phases of the system Co–Fe–Mn–O at 1200°C have been investigated with regard to their relation to the phase equilibria between these phases. To describe the thermodynamics of the spinel phase, a sub-lattice model, based on the cation distribution of 2+ and 3+ ions between octahedral and tetrahedral sites has been used. In the modelling, the influence of deviations from stoichiometry has been taken into account for the rock-salt structure phase. A set of thermodynamic parameters has been derived which allows the calculation of the compositions of the spinel and rock-salt structure phases at equilibrium as a function of oxygen partial pressure at 1200°C. The model also permits the calculation of the cation distribution in the ternary spinel phase at all compositions.

Keywords: Thermodynamics, Co–Fe–Mn–O system, spinel, mixed oxides.

1. INTRODUCTION

By modelling the thermodynamic properties of solutions, it is often possible to gain insight into their structure. At the same time, the models permit a consistent means of smoothing, interpolating and extrapolating data. Phase diagrams are a form of thermodynamic data, since they represent the conditions for minimum free energy of the system. In this paper, we shall propose models for the oxide phases with the rock-salt and spinel structures in the Co–Fe–Mn–O system at 1200°C and a hydrostatic pressure of 1 atm. By minimizing the free energy of the system, the phase stability limits of each phase can be calculated from the models and compared to experimental values. The free energies of the oxide phases depend on their cationic composition and on their oxygen content. For the determination of free energy minima it is critical to formulate appropriately the free energy of each phase as a function of its chemical composition. For spinels in which ions can occur in different coordinations, this requires that the dependence of the free energy on the internal cation distribution also be formulated.

Oxides with the rock-salt structure are based on a face-centered cubic lattice of oxygen atoms in which all octahedral interstices are filled by cations. Oxides with the spinel structure are based on the same oxygen packing. However only 1/2 of the octahedral interstices and 1/8 of the available tetrahedral interstices are filled by cations. Details of the spinel structure are reviewed, for example, in [1]. At thermodynamic equilibrium, cations and point defects are distributed among the different coordinations in such a way that the free energy of the crystal is minimized. Different factors which are sensitive to this distribution contribute to the crystal's free energy [2]. First, the crystal's lattice energy, including the Madelung energy and a repulsive energy term, is important. Second, factors such as crystal field stabilization, ligand field stabilization, and the Jahn–Teller effect cannot be ignored, especially if transition metal cations are present. Lattice polarization may also have to be considered, especially in view of fast electron exchanges between transition metal cations. Ordering on individual sub-lattices may also cause energy changes. Furthermore, in general, the oxygen sub-lattice is not densely packed. As a consequence, the lattice parameter, a, and also the so-called oxygen parameter, u, which is used to denote exactly the positions of oxygen ions (see [1, 3]) depend on the ion distribution. In principle, this has to be taken into account when free energy changes of different origin are formulated and/or calculated.

Unfortunately, it is extremely difficult to formulate quantitatively the contributions to the free energy

of spinels resulting from the factors discussed above. To date, this problem has not been satisfactorily solved. Different models have been proposed to treat quantitatively the cation distribution in spinels. However, none of them takes all these factors into account. Therefore, all models proposed so far [4–14] have only limited applicability, depending on the specific system considered and on the factors ignored by the specific model.

The exchange of differently charged cations between the octahedral and tetrahedral cation sites changes the charge distribution. Due to the nondense nature of the oxygen packing, the interionic distances vary if cations of different sizes are exchanged between different types of sites. Both charge distribution and changes in interaction distances affect the value of the electrostatic energy [15]. Hence the lattice energy (with the largest contribution from the Coulomb interactions) changes with the distribution of cations. If this variation is small compared to the contribution from the stabilization of ions due to crystal field effects, the latter effect determines the equilibrium distribution of ions. Models emphasizing only lattice energy considerations [9–14] and some based exclusively on crystal field stabilization effects [5–8] have been proposed to model the cation distribution in spinels. The exact calculation of lattice energies is a problem due to a lack of compressibility data for quantifying repulsive interactions, and the great difficulty involved in quantifying the effect of lattice polarizations and of energy changes due to ordering of cations on different sub-lattices. The distribution of ions with different valence states is governed both by the exchange of ions between the two sites and electron exchange reactions between ions. If compounds or solid solutions contain transition metals ions with different charge states in comparable concentrations, fast electron exchange may affect the free energy of mixing. In such cases, both of the aforementioned models may fall short of an appropriate physical picture of the cation distribution.

Early attempts to model cation distribution were based on treating it as a simple chemical equilibrium between ions on octahedral and tetrahedral sites [4]. Enthalpies for the exchange of ions between the two sites, derived from empirical site preference energies [5–7] of individual ions, were used to model cation distributions. By assuming the exchange enthalpies to be independent of the concentrations of ions on each of the sites, the model was extended to binary spinel solid solutions. With this principle, and assuming the non-configurational entropy to be small, Navrotsky [8] and Pelton *et al.* [16] modelled cation distributions in A_3O_4–B_3O_4 solid solutions, where A, B = Co, Fe and Mn. In a later study, O'Neill and Navrotsky [9] added a semi-empirical nonlinear term to the variation of enthalpy with cation distribution. With a few exceptions, the cation distribution of many spinels and of spinel solid solutions can be fitted by this empirical model. Further extensions have been proposed, based on a second degree Taylor series expansion, to model the trends in the cation distribution of multicomponent systems [12–14]. However, proof is lacking that these models appropriately take into account the physics governing the cation distribution.

In this study, the free energy dependence of the Co_3O_4–Fe_3O_4–Mn_3O_4 spinel solid solution on composition is modelled on the basis of the distribution of different cations with 2+ and 3+ valence states between octahedrally and tetrahedrally coordinated cation sites. In view of the complexity of the system considered and the open questions with regard to the appropriate modelling of the cation distribution in spinels, a simple semi-empirical approach has been selected which provides a set of equations useful for modelling the cation distribution. It is assumed that the distribution of ions is governed by the difference of site preference enthalpies of ions between tetrahedral and octahedral coordination. This implies that the enthalpy of disordering is considered to be independent of composition and sub-lattice population. Deviations are formally treated by introducing empirical excess enthalpies. This approach has been already used to model the cation distribution of the constituent transition metal oxides and of their quasi-binary solid solutions of the system considered here [16]. In the present article, this approach is extended to quasi-ternary spinel solid solutions. For this purpose, a so-called sub-lattice model [17–20], originally developed for modelling molten salt solutions, has been modified. In this model, spinel solid solutions are considered as a mixture of spinel-like, pseudo-components, involving two octahedral and one tetrahedral cation site per molecule. The free energy of the system is obtained by summing the free energies of the pseudo-components and the entropies of cation mixing on the octahedral and tetrahedral sub-lattices. Nonstoichiometry in the spinel phase is assumed to have a negligible effect on the cation distribution and overall free energy.

Once the free energies of the spinel and rock-salt structure phases have been formulated as a function of composition, the free energies of combinations of these two phases as a function of composition and oxygen activity can be minimized to determine the compositions coexisting at different oxygen partial pressures. Finally, through comparison with experimental results, adjustments of the model in the form of empirical excess energy parameters, can be made.

2. EFFECT OF NONSTOICHIOMETRY ON THE FREE ENERGY OF OXIDE SOLID SOLUTIONS

The free energy of a nonstoichiometric phase is a function of defect concentrations and composition. When the equilibrium between two phases with large differences between their degrees of nonstoichiometry is considered the point defect formation in the more nonstoichiometric phase has the most significant effect on the equilibrium.

The system considered here contains three different transition metals: Co, Fe and Mn. Their stable oxides with the spinel [21–23] and rock-salt structures [24–27] are well known to be nonstoichiometric. For the present calculation of phase equilibria between $(Co, Fe, Mn)_{1-\Delta}O$ and $(Co, Fe, Mn)_{3-\delta}O_4$, in principle the degrees of nonstoichiometry of the coexisting spinel and rock-salt structure phases must be known. However, the deviation from stoichiometry in the spinel phase δ can be ignored in the calculations because the δ-values are sufficiently small. Only Δ in the rock-salt structure phase is important. From the literature it is well known that the deviation from stoichiometry, Δ, in $Fe_{1-\Delta}O$ varies between about 0.05 and 0.15 at 1200°C [24]. Investigations of the nonstoichiometry in $Mn_{1-\Delta}O$ have yielded a range of deviation from stoichiometry from ~ 0 to about 0.06 at 1200°C [25]. In $Co_{1-\Delta}O$ the maximum deviation from stoichiometry at 1200°C is about 0.01 [26, 27]. To determine quantitatively the effect of the nonstoichiometry on the free energy of $(Co, Fe, Mn)_{1-\Delta}O$ with varying oxygen activity and cationic composition, Δ must be known in the entire stability region of the rock-salt structure phase. Unfortunately, such data are lacking. Therefore, simplifying assumptions must be made. The simplest approach of this nature has been reported in [16]. There it has been assumed that variations in the oxygen content, given by $1/(1-\Delta)$, in $Mn_{1-\Delta}O$ and $Co_{1-\Delta}O$ are negligible compared to that in $Fe_{1-\Delta}O$ at 1200°C. Furthermore, it was assumed that in quasi-binary phases the oxygen content in $(Fe_yA_{1-y})_{1-\Delta}O \approx y \cdot$ (oxygen content in $Fe_{1-\Delta}O$) at constant temperature and oxygen activity, and analogously, in quasi-ternary systems the oxygen content in $(A_xFe_yB_{1-x-y})_{1-\Delta}O \approx y \cdot$ (the oxygen content in $Fe_{1-\Delta}O$). However, recently it has been shown for the quasi-binary phases $(Fe_yMn_{1-y})_{1-\Delta}O$ and $(Co_xFe_y)_{1-\Delta}O$ $(x+y=1)$, that the oxygen content is not exactly linearly dependent on y, and that the effect of this nonlinearity on the free energy cannot be neglected if accurate phase diagram calculations are desired [28, 29].

Consider $1/(1-\Delta)$ moles of the binary solid solution $(Fe_yA_{1-y})_{1-\Delta}O$. The Gibbs energy of this solution is:

$$
\begin{aligned}
{}^{\circ}G^{ex}_{a_{O_2}} &= y \cdot \mu_{FeO} + (1-y) \cdot \mu_{AO} + \frac{\Delta}{2 \cdot (1-\Delta)} \cdot \mu_{O_2} \\
&= y \cdot \mu^{\rho}_{FeO} + (1-y) \cdot \mu^{\rho}_{AO} \\
&\quad + R \cdot T \cdot [y \cdot \ln y + (1-y) \cdot \ln(1-y)] \\
&\quad + \frac{\Delta}{2 \cdot (1-\Delta)} \cdot \mu_{O_2} + G^{ex}_{FeA}, \qquad (1)
\end{aligned}
$$

where μ_{FeO} and μ_{AO} are chemical potentials, μ^{ρ}_{FeO} and μ^{ρ}_{AO} are their values in $Fe_{1-\Delta}O$ and $A_{1-\Delta}O$ at a constant oxygen activity, a_{O_2} $(=P_{O_2}/P^{\circ}$; $P^{\circ}=1$ bar), and G^{ex}_{FeA} is an excess Gibbs energy. $\mu_{O_2}(=2\mu_O)$ is the chemical potential of O_2 (and μ_O that of O).

A simple expression describing the deviation from stoichiometry, Δ, in $Fe_{1-\Delta}O$ as a function of oxygen activity and temperature is available [30]:

$$
x_O = \frac{1}{2-\Delta} = \frac{\log a_{O_2} - \dfrac{A_3}{T} - A_4}{\dfrac{A_1}{T} + A_2} \qquad (2)
$$

with $A_1 = -35{,}658$ K, $A_2 = 128.48$, $A_3 = -10{,}096$ K and $A_4 = 58.373$. This expression can be used with the Gibbs–Duhem equation, applied to the two-component system consisting of FeO and excess oxygen, to calculate μ^{ρ}_{FeO} in $Fe_{1-\Delta}O$ as a function of oxygen activity:

$$
x_O \cdot d\mu_O + x_{FeO} \cdot d\mu^{\rho}_{FeO} = 0 \qquad (3)
$$

$$
d\mu^{\rho}_{FeO} = -\frac{x_O}{x_{FeO}} \cdot \mu_O = -\frac{\Delta}{1-\Delta} \cdot d\mu_O \qquad (4)
$$

$$
\mu^{\rho}_{FeO}(a''_{O_2}) - \mu^{\rho}_{FeO}(a'_{O_2}) = -\frac{R \cdot T}{2} \times \int_{a'_{O_2}}^{a''_{O_2}} \frac{\Delta}{1-\Delta} \cdot d\ln a_{O_2} \qquad (5)
$$

If we select $Fe_{1-\Delta}O$ in equilibrium with Fe as the standard state, the lower limit of the integral becomes $a'_O(Fe/Fe_{1-\Delta}O)$ and $\mu^{\rho}_{FeO}(a'_O) = 0$. This permits the calculation of the activity of FeO at any oxygen activity with respect to the selected standard state by substitution of eqn (2) into eqn (5). It is worth noting that for the calculations it is necessary to extrapolate eqn (2) to oxygen activities beyond that of the $Fe_{1-\Delta}O/Fe_{3-\delta}O_4$ equilibrium. An analogous approach is also used to calculate $\mu^{\rho}_{MnO}(a''_{O_2})$. The dependence of Δ in $Mn_{1-\Delta}O$ on a_{O_2} is obtained by using experimental data reported in [25]. For $Co_{1-\Delta}O$, recent data for Δ are available from [27].

Values of the excess Gibbs energies G^{ex}_{FeCo} and G^{ex}_{FeMn} in eqn (1) were obtained from experimental data on the nonstoichiometry of the quasi-binary $(Fe_yMn_{1-y})_{1-\Delta}O$ [28] and $(Co_xFe_y)_{1-\Delta}O$ $(x+y=1)$ [29, 31] phases as a function of a_{O_2} and cationic composition. Empirical expressions for G^{ex}_{FeCo} and G^{ex}_{FeMn} are reported in Table 1. It may be shown that if the approximation that the oxygen content in $(Fe_yMn_{1-y})_{1-\Delta}O = y \cdot$ (oxygen content in $Fe_{1-\Delta}O$) were true, then the excess Gibbs energies in Table 1 would be independent of a_{O_2} and would depend only upon the metal ratios. In reality, a significant oxygen activity dependence is observed.

For $1/(1-\Delta)$ moles of the ternary solid solution $(Co_xFe_yMn_{1-x-y})_{1-\Delta}O$, the following expression for the Gibbs energy was used:

$$G^{ex}_{a_{O_2}} = x \cdot \mu^{\rho}_{CoO} + y \cdot \mu^{\rho}_{FeO} + (1-x-y) \cdot \mu^{\rho}_{MnO} + R \cdot T \cdot [x \cdot \ln x + y \cdot \ln y + (1-x-y) \times \ln(1-x-y)] + (1-x)^2 \cdot G^{ex}_{FeMn} + (1-(1-x-y))^2 \cdot G^{ex}_{CoFe} + (1-y)^2 \times G^{ex}_{CoMn} + \frac{\Delta}{2 \cdot (1-\Delta)} \cdot \mu_{O_2}, \quad (6)$$

where the binary excess terms G^{ex}_{ij} are calculated from Table 1 at the same molar ratio i/j as at the ternary composition point. This approximation for the excess free energy of the ternary phase is known as the Kohler approximation [32] and is based on an extension of simple regular solution theory. For a large number of simple ionic phases, it has been found that this approximation gives very good results in all cases. Due to the lack of experimental data, G^{ex}_{CoMn} was assumed to be zero in eqn (6). In conclusion, eqn (6) is the best possible approximation for the change of the free energy in the quasi-ternary oxide solid solution $(Co_xFe_yMn_{1-x-y})_{1-\Delta}O$ with the currently available data.

Table 1. Excess free energy terms for rock-salt structure oxide solid solutions at different oxygen activities [28, 29]

(a) $(Co_xFe_yMn_{1-x-y})_{1-\Delta}O$ with $x = 0$

$\log_{10} a_{O_2}$	G^{E}_{FeMn} (kJ/mol)
−6	$-0.06 \cdot y \cdot (1-y) + 15.58 \cdot y \cdot (1-y)^2$
−7	$4.57 \cdot y \cdot (1-y) + 9.92 \cdot y \cdot (1-y)^2$
−8	$3.71 \cdot y \cdot (1-y) + 10.54 \cdot y \cdot (1-y)^2$

(b) $(Co_xFe_yMn_{1-x-y})_{1-\Delta}O$ with $x+y=1$

$\log_{10} a_{O_2}$	G^{E}_{CoFe} (kJ/mol)
−2	$-15.8 \cdot x \cdot (1-x) + 29.68 \cdot x^2 \cdot (1-x)$
−4	$-12.9 \cdot x \cdot (1-x) + 25.12 \cdot x^2 \cdot (1-x)$
−6	$-11.3 \cdot x \cdot (1-x) + 35.46 \cdot x^2 \cdot (1-x)$
−8	$1.44 \cdot x \cdot (1-x) + 15.50 \cdot x^2 \cdot (1-x)$

In the spinel phase, the maximum deviation from stoichiometry is observed at high oxygen activities in magnetite, $Fe_{3-\delta}O_4$. At 1200°C, δ in $Fe_{3-\delta}O_4$ varies between $-3.3 \cdot 10^{-3}$ and $4.9 \cdot 10^{-2}$ [22]. At equilibrium with the rock-salt structure phase, the negative value of δ is due to iron interstitials. As mentioned earlier, for our analysis we assume that the nonstoichiometry of the spinel phase does not significantly affect the phase equilibria. In the case of pure $Fe_{3-\delta}O_4$ this assumption seems reasonable since the fraction of vacant cation sites does not exceed ~0.016 and that of cations on interstitial sites does not exceed ~0.0011. In the quasi-ternary system, this assumption is even better. Recent measurements of the nonstoichiometry in spinel solid solutions of the type $(Co, Fe, Mn)_{3-\delta}O_4$ show that the deviation from stoichiometry significantly decreases with decreasing $Fe_{3-\delta}O_4$ content [23]. For the sake of simplicity, in the following discussion, spinel compounds will be denoted as Me_3O_4 with the understanding that δ is assumed to be negligibly small.

3. SUBLATTICE MODEL

As mentioned above, due to the complexity involved in the exact treatment of the cation distribution in the solid solution $(Co_xFe_yMn_{1-x-y})_3O_4$, a simple, semi-empirical approach is used. The cation distribution is assumed to be governed by various site- and charge-exchange reactions of which the equilibrium constants are independent of composition [8, 16]. It is also assumed that the cations on each sublattice are randomly distributed.

For example, the cation distribution in Fe_3O_4 may be represented as

$$(Fe^{2+}_{1-z}Fe^{3+}_{z})[Fe^{2+}_{z}Fe^{3+}_{2-z}]O_4. \quad (7)$$

Ions in the round parentheses are located on tetrahedral sites and those in the square ones on octahedral sites. The cation distribution is determined by the equilibrium constant of the "site exchange reaction":

$$Fe^{2+}_{A} + Fe^{3+}_{B} \rightleftarrows Fe^{2+}_{B} + Fe^{3+}_{A}. \quad (8)$$

The subscripts A and B refer to tetrahedral and octahedral sites, respectively. The molar Gibbs energy change of this exchange reaction is:

$$\Delta G^{ex}_{FeFe} = [\epsilon(Fe^{2+}_{B}) - \epsilon(Fe^{2+}_{A})] - [\epsilon(Fe^{3+}_{B}) - \epsilon(Fe^{3+}_{A})]. \quad (9)$$

The terms $\epsilon(ion^{n+}_{site})$ are the molar energies associated with the differently charged ions on the sites indicated. The bracketed terms, $[\epsilon(Fe^{2+}_{B}) - \epsilon(Fe^{2+}_{A})]$ and

$[\epsilon(Fe_B^{3+}) - \epsilon(Fe_A^{3+})]$, are called the octahedral site preference energies of Fe^{2+} and Fe^{3+} ions, respectively. If the ϵ-terms are independent of composition, then one can write:

$$K = \exp\left(-\frac{\Delta G^{ex}_{FeFe}}{R \cdot T}\right) = \frac{\alpha^2}{(1-\alpha)\cdot(2-\alpha)}. \quad (10)$$

By solving eqn (10) for α, the cation distribution can be calculated.

For the quasi-ternary spinel solid solution of interest, a set of independent exchange reactions can be formulated in terms of the unknown concentrations of ions in the two sub-lattices. The cation distribution can be written as

$$(Co_a^{2+}Co_b^{3+}Fe_c^{2+}Fe_d^{3+}Mn_e^{2+}Mn_f^{3+}) \times [Co_g^{2+}Co_h^{3+}Fe_i^{2+}Fe_j^{3+}Mn_k^{2+}Mn_l^{3+}]O_4. \quad (11)$$

Site, charge and mass balances yield:

$$a + b + c + d + e + f = 1, \quad (12)$$

$$g + h + i + j + k + l = 2, \quad (13)$$

$$2\cdot(a + c + e + g + i + k) + 3\cdot(b + d + f + h + j + l) = 8, \quad (14)$$

$$e + f + k + l = x_{Mn_3O_4} = 1 - x - y, \quad (15)$$

$$a + b + g + h = x_{Co_3O_4} = x, \quad (16)$$

$x_{Mn_3O_4}$ and $x_{Co_3O_4}$ are the overall mole fractions of Mn_3O_4 and Co_3O_4. Seven independent internal equilibria can be formulated:

$$Fe_A^{2+} + Fe_B^{3+} \rightleftarrows Fe_B^{2+} + Fe_A^{3+}$$

$$\Delta G^{ex}_{FeFe} = -R\cdot T\cdot \ln\left(\frac{i\cdot d}{c\cdot f}\right), \quad (17)$$

$$Mn_A^{2+} + Mn_B^{3+} \rightleftarrows Mn_B^{2+} + Mn_A^{3+}$$

$$\Delta G^{ex}_{MnMn} = -R\cdot T\cdot \ln\left(\frac{k\cdot f}{e\cdot l}\right), \quad (18)$$

$$Fe_A^{2+} + Mn_B^{3+} \rightleftarrows Fe_B^{2+} + Mn_A^{3+}$$

$$\Delta G^{ex}_{FeMn} = -R\cdot T\cdot \ln\left(\frac{i\cdot f}{c\cdot l}\right), \quad (19)$$

$$Co_A^{2+} + Co_B^{3+} \rightleftarrows Co_B^{2+} + Co_A^{3+}$$

$$\Delta G^{ex}_{CoCo} = -R\cdot T\cdot \ln\left(\frac{g\cdot b}{a\cdot h}\right), \quad (20)$$

$$Co_A^{2+} + Mn_B^{3+} \rightleftarrows Co_B^{2+} + Mn_A^{3+}$$

$$\Delta G^{ex}_{CoMn} = -R\cdot T\cdot \ln\left(\frac{g\cdot f}{a\cdot l}\right), \quad (21)$$

$$Fe_B^{2+} + Mn_B^{2+} \rightleftarrows Fe_B^{2+} + Mn_B^{3+}$$

$$\Delta G^{red}_{FeMn} = -R\cdot T\cdot \ln\left(\frac{i\cdot l}{j\cdot k}\right), \quad (22)$$

$$Fe_B^{3+} + Co_B^{2+} \rightleftarrows Co_B^{3+} + Fe_B^{2+}$$

$$\Delta G^{red}_{FeCo} = -R\cdot T\cdot \ln\left(\frac{h\cdot i}{j\cdot g}\right). \quad (23)$$

Equations (17–21) are site-exchange equilibria, while eqns (22) and (23) are redox reactions on the octahedral sub-lattice. Other equilibria, such as redox reactions on the tetrahedral sub-lattice, can be obtained by linear combinations of these equations.

Site-exchange Gibbs energies, ΔG^{ex}, have been estimated from crystal field theory [5] and from an assessment of thermodynamic and spectroscopic data [6]. Redox Gibbs energies, ΔG^{red}, have been estimated from thermodynamic data [8]. In an earlier publication by one of the authors [16], values of ΔG^{ex} and ΔG^{red} for the quasi-binary spinel solid solutions Fe_3O_4–Mn_3O_4, Fe_3O_4–Co_3O_4 and Co_3O_4–Mn_3O_4 were deduced from assessments of phase diagrams. By using these ΔG-values in eqns (17–21), and solving eqns (12–23) simultaneously, cation distributions can be determined. A method to obtain an exact solution of this problem was presented earlier for the quasi-binary systems Fe_3O_4–Mn_3O_4, Fe_3O_4–Co_3O_4 and Co_3O_4–Mn_3O_4 [16]. However, this approach is very complex and tedious, even for the quasi-binary systems.

For the quasi-ternary spinel phase $(Co_xFe_yMn_{1-x-y})_{3-\delta}O_4$ there are (at least) six types of ions, each of which can reside on two sub-lattices. For the solution of eqns (12–23), a more general numerical approach is proposed which is based on the concepts of the sub-lattice model developed by Blander and Yosim [17] for reciprocal ternary molten salt solutions and formalized by one of the authors [18] for multicomponent systems. The sub-lattice model has been used to model systems other than molten salts [19].

For the application of the sub-lattice model to the spinel solid solution $(Co_xFe_yMn_{1-x-y})_{3-\delta}O_4$, neutral "pseudo-components" could be defined in which three discrete ions are distributed on one tetrahedrally and two octahedrally coordinated cation sites in a molecular unit. For $(Co_xFe_yMn_{1-x-y})_{3-\delta}O_4$, 45 different neutral pseudo-components could be formulated of which not all are independent from each

other, i.e. cannot be obtained by a combination of other neutral pseudo-components. However, the calculations performed have not been based on direct combinations of neutral, independent pseudo-components. Instead, because a suitable general computer program had already been developed earlier by two of the authors, the modelling of the spinel solid solution has been based on the combination of pseudo-components some of which are electrically charged. In each of these pseudo-components the tetrahedral and octahedral sites are each occupied exclusively by one kind of ion. That is, there are 36 pseudo-components of the type $\{(A^{n+})[B^{m+}B^{m+}]O_4\}^{(2m+n-8)+}$. Combinations of pseudo-components are always made so that overall electroneutrality is maintained. For example, by combining the charged pseudo-components $\{(A^{3+})[B^{3+}B^{3+}]O_4\}^{+1}$ and $\{(A^{3+})[B^{2+}B^{2+}]O_4\}^{-1}$ in equal amounts a neutral unit is obtained. It can be shown that this treatment is formally equivalent to the method involving only neutral pseudo-components.

As in eqn (9), energies ϵ are defined which are associated with the ions on each sub-lattice. In principle, these energies correspond to standard values of electrochemical potentials. However, because only neutral combinations are considered later, the electrical terms then cancel out. Therefore they are not formulated explicitly. The standard molar Gibbs energy of a pseudo-component is then the sum of the energies of its ions. For example,

$$G^0_{(Fe^{3+})[Mn^{2+}+Mn^{2+}]O_4} = \epsilon(Fe^{3+}_A) + 2\cdot\epsilon(Mn^{2+}_B), \quad (24)$$

and analogously for all other pseudo-components considered.

The Gibbs energy of a mole of the solid solution $(Co_xFe_yMn_{1-x-y})_{3-\delta}O_4$ at any composition is given as:

$$G = \sum_{m=1}^{6}\sum_{n=1}^{6} x_{m(A)}\cdot x_{n(B)}\cdot G^0_{(m)[nn]O_4} + R\cdot T\left(\sum_{m=1}^{6} x_{m(A)}\cdot \ln x_{m(A)} + 2\cdot\sum_{n=1}^{6} x_{n(B)}\cdot \ln x_{n(B)}\right) + G^E. \quad (25)$$

The summations are over all six m-ions on the tetrahedral A sub-lattice and all six n-ions on the octahedral B sub-lattice. $x_{m(A)}$ and $x_{n(B)}$ are the fractions of A sites occupied by m ions and of B sites occupied by n ions, respectively. G^E is an excess Gibbs energy.

The Gibbs energies $G^0_{(m)[nn]O_4}$ of the pseudo-components can be evaluated from the Gibbs energies, ΔG^{ex} and ΔG^{red}, of the exchange and redox reactions.

With no loss in generality, one can arbitrarily select for the standard states

$$\epsilon(Fe^{2+}_A) = \epsilon(Fe^{2+}_B) = \epsilon(Fe^{3+}_B) = C_1, \quad (26)$$

$$\epsilon(Mn^{3+}_B) = C_2, \quad (27)$$

and

$$\epsilon(Co^{3+}_B) = C_3. \quad (28)$$

C_1, C_2, C_3 are constants. For the $(Fe_yMn_{1-y})_3O_4$ solid solution based on reactions (17) to (19) and (22) one can write

$$\Delta G^{ex}_{FeFe} = \epsilon(Fe^{3+}_A) - C_1 \quad (29)$$

$$\Delta G^{ex}_{MnMn} = \epsilon(Mn^{2+}_B) + \epsilon(Mn^{3+}_A) - \epsilon(Mn^{2+}_A) - C_2 \quad (30)$$

$$\Delta G^{ex}_{FeMn} = \epsilon(Mn^{3+}_A) - C_2 \quad (31)$$

$$\Delta G^{red}_{FeMn} = -\epsilon(Mn^{2+}_B) + C_2. \quad (32)$$

Similar independent equilibria can be formulated for the $(Co_xFe_y)_3O_4$ $(x+y=1)$ solid solution.

$$\Delta G^{ex}_{CoCo} = \epsilon(Co^{2+}_B) + \epsilon(Co^{3+}_A) - \epsilon(Co^{2+}_A) - C_3 \quad (33)$$

$$\Delta G^{ex}_{FeCo} = \epsilon(Co^{3+}_A) - C_3 \quad (34)$$

$$\Delta G^{red}_{FeCo} = -\epsilon(Co^{2+}_B) + C_3. \quad (35)$$

From eqns (26) to (35), all energies ϵ can be evaluated. Hence, the G^0 values for all 36 pseudo-components can be calculated. For example, from eqns (24), (29) and (32):

$$G_{(Fe^{3+})[Mn^{2+}Mn^{2+}]O_4} = \Delta G^{ex}_{FeFe} + C_1 + 2\times(C_2 - \Delta G^{red}_{FeMn}). \quad (36)$$

Inserting values for $G^0_{(m)[nn]O_4}$ into eqn (25), and introducing an appropriate expression for G^E as a function of composition, we find the site fractions $x_{m(A)}$ and $x_{n(B)}$ which minimize G subject to the constraints of the overall mole fractions of the real components ($x_{Fe_3O_4}$, $x_{Mn_3O_4}$ and $x_{Co_3O_4}$) and of the overall charge neutrality. If G^E is assumed to be zero, this treatment is formally equivalent to the solution of eqns (12–23). It can be shown that the calculated values of $x_{m(A)}$ and $x_{n(B)}$ (that is, the cation distribution) are independent of the arbitrary constants C_1, C_2 and C_3.

Standard numerical techniques of calculating constrained minima can be used, and the procedure can be generalized to any number of components. In the present case we have used the EQUILIB program of the F*A*C*T thermodynamic computer system which incorporates the general constrained Gibbs energy minimization routines SOLGASMIX [33, 34].

Although the cation distribution is independent of the constants C_1, C_2 and C_3, values must be assigned to these constants if equilibria between the spinel phase and other phases (such as the rock-salt structure phase) are to be calculated. Taking first pure Fe_3O_4, we solve for the cation distribution by minimizing G in eqn (25). Setting $C_1 = 0$, this then gives $G^0_{Fe_3O_4}(C_1 = 0)$. C_1 can then be calculated from the relation $G^0_{Fe_3O_4} = (G^0_{Fe_3O_4}(C_1 = 0) + 3C_1)$, where $G^0_{Fe_3O_4}$ is the experimental value, relative to the standard state of the elements at 298 K, which can be found in standard thermodynamic tables. Repeating the procedure for pure Mn_3O_4 and Co_3O_4 permits C_2 and C_3 to be obtained.

In a previous investigation [16], good fits to the equilibrium data for the Fe_3O_4–Mn_3O_4, Fe_3O_4–Co_3O_4 and Co_3O_4–Mn_3O_4 systems were obtained for a range of temperatures and oxygen activities with $G^E = 0$ in eqn (25). However, with the correct inclusion of the nonstoichiometry in oxide solid solutions with the rock-salt structure, at least at 1200°C, it is necessary to include a set of small empirical excess energy terms to obtain a good fit of the experimental data. These excess energy terms may be treated formally as arising from cation–cation interactions. However, so many interactions are possible that there is no way to determine, on the basis of the available data, which interactions give rise to the excess terms. Hence the choice of the exact form of the excess terms is rather arbitrary. For example, if we consider that A–B interactions between a cation on an A site and a cation on a B site are responsible for the excess terms, then we could add excess terms such as $a \cdot x_{i(A)} \cdot x_{i(B)}$ to eqn (25) where a is an adjustable parameter. If, instead, we consider A–A and B–B interactions between cations on the same sub-lattice, then we could add excess terms such as $a \cdot x_{i(A)} \cdot x_{j(A)}$. Either choice gives good results.

In the present case, we arbitrarily decided to treat the binary excess terms as being due to interactions on the same sub-lattice. Taking as example the Fe_3O_4–Co_3O_4 binary system, we further assume that all Fe–Co interactions on the same sub-lattice have the same energy regardless of the ionic charge and regardless of the sub-lattice. "Regular" and higher order binary excess terms can then be written as:

$$G^E_{FeCo} = \sum_{\substack{i = Fe^{2+}, Fe^{3+} \\ j = Co^{2+}, Co^{3+}}} \sum_{m,n} a_{mn} \cdot \left[\frac{x^m_{i(A)} \cdot x^n_{j(A)}}{(x_{i(A)} + x_{j(A)})^{m+n-2}} \times (1 - x_{Mn^{2+}_B} - x_{Mn^{3+}_B}) + \frac{x^m_{i(B)} \cdot x^n_{j(B)}}{(x_{i(B)} + x_{j(B)})^{m+n-2}} \times (1 - x_{Mn^{2+}_A} - x_{Mn^{3+}_A}) \right]. \quad (37)$$

As an abbreviated notation, for $(Co_xFe_yMn_{1-x-y})_3O_4$ with $(x + y) = 1$, the binary excess energy terms can be written as:

$$G^{ex}_{FeCo} = \sum_{m,n} a_{mn} \cdot x^m \cdot y^n. \quad (38)$$

It must be stressed, however, that eqn (38) is only a compressed notation. Equation (37) is the full form, a_{11} can be called a "regular" adjustable parameter, a_{12} and a_{21} are "sub-regular" parameters, etc. Although eqn (37) contains many terms, there are only a very few parameters necessary to fit the data for the Fe_3O_4–Co_3O_4 system. Analogous expressions can be formulated for the excess energies in the Fe_3O_4–Mn_3O_4 and Mn_3O_4–Co_3O_4 systems. In any of the binary systems, no more than one adjustable parameter was required to satisfactorily fit the available data. The binary excess terms are then added together to give the ternary G^E term in eqn (25). This can be shown to be very similar to the Kohler approximation [32], discussed earlier, for estimating the effect of a third component upon binary interactions. Although a simpler equation could be used in the present case, the consistent use of the Kohler equation permits us to write very general computer programs for a wide variety of solution types. Again, it should be stressed that the excess terms are small, and are necessary only when precise curve fitting of experimental data is desired. It is not intended that physical significance be attached to these parameters, and so the form of the equations used for G^E can be chosen with some latitude.

Ternary excess terms can also be included in eqn (25). These terms must be zero in all three binary sub-systems. In the present case, only one small ternary excess term was included. This term was chosen arbitrarily, as being due to triplet Co–Fe–Mn cation interactions, with all such interactions having

the same energy regardless of the sites occupied by the ions. That is:

$$G^{E}_{FeMnCo} = \sum_{\substack{i=Fe^{2+},Fe^{3+}\\ j=Mn^{2+},Mn^{3+}\\ k=Co^{2+},Co^{3+}}} \sum_{\substack{P=A,B\\ Q=A,B\\ R=A,B}} a \times X_{i(P)} \cdot X_{j(Q)} \cdot X_{k(R)}, \quad (39)$$

where a is the single adjustable parameter.

The sub-lattice model can be generalized to apply to other multicomponent ceramic phases with two cation sub-lattices (such as $(A^{2+})_2(B^{4+})O_4$ spinels, pseudobrookite phases, ilmenite phases, etc.). General computer routines have been written which can be used for all such solutions.

4. PROCEDURE

With the free energy of the spinel and rock-salt structure phases formulated as described in the previous sections, minimization of the Gibbs energy of a combination of the phases is carried out using the EQUILIB program of the F*A*C*T system. This program incorporates the numerical techniques of SOLGASMIX for calculating Gibbs energy minima for a multicomponent system.

The standard free energies of the spinel-like pseudo-components are calculated from the site energies for individual ions on the octahedral and tetrahedral coordinations using eqn (24). For calculating phase equilibria between the spinel and rock-salt structure phases, the constants C_1, C_2 and C_3 (see eqns (26) to (28)) have to be calculated, as discussed above. The standard free energies used for this purpose are listed in Table 2. The expression for the formation energy for Co_3O_4 has been derived by fitting experimental data available from the literature [36–40] for the $Co_{1-\Delta}O/Co_{3-\delta}O_4$ phase equilibrium at one atm total pressure including recent information on this equilibrium at higher total pressures [41]. For the oxygen activity at the $Co_{1-\Delta}O/Co_{3-\delta}O_4$ equilibrium we obtained

$$\log_{10} a_{O_2} = 20.569 - \frac{22{,}730}{T/K} - 1.425 \times 10^{-6} \times T/K^2. \quad (40)$$

For the quasi-binary rock-salt structure oxide solid solutions, the free energy of the phase as a function of oxygen partial pressure and composition, taking into account the nonstoichiometry of the solid solution, has been calculated as discussed earlier (see also [28, 29]). In both the quasi-binary and the quasi-ternary systems, the free energy minimization is performed at different oxygen activities in order to obtain the compositions of the spinel and rock-salt structure oxides in equilibrium with each other.

First, free energy minimizations were carried out for the three quasi-binary phases. The calculated phase equilibria between the spinel and rock-salt structure phases with varying oxygen activity then were compared with the available experimental data. The site preference energy values were varied to obtain a best fit of the experimental rock-salt structure phase boundaries in all the three quasi-binary phases. Guidelines for the effect of site preference energies on the quasi-binary phase equilibria are reported in detail in [16]. They were used to obtain a set of site preference energies that best fit the measured phase boundaries. Then, this set of site preference energies was used for further calculations in the quasi-ternary phase. Small excess energy terms were included in this model to improve the fit of the experimental data in the quasi-binary (see eqn (38)) and in the quasi-ternary solid solutions (see eqn (39)). The phase equilibria calculated for the quasi-binary systems are compared with the information available in the literature [28, 29, 42] and those calculated for the quasi-ternary solid solution are compared with recent experimental data [43]. A semi-quantitative picture of the trends in the cation distribution in the binary and ternary spinel phases was obtained from the site preference energies selected.

5. RESULTS AND DISCUSSION

The phase stability limits in quasi-binary systems are reported in $\log a_{O_2}$ versus composition phase diagrams for constant temperature and total pressure. These diagrams are topologically similar to binary temperature–composition phase diagrams. Although these diagrams do not show deviations from stoichiometry at equilibrium, they are much more convenient to handle than the three-dimensional plots which would be required to do this. In the quasi-ternary system, due to the addition of one composition variable, the two-phase region between the spinel and rock-salt structure phases would in

Table 2. Thermodynamic data used in the calculations

Reaction	ΔG (at 1200°C) [kJ/mol]	Ref.
$3FeO + 0.5O_2 = Fe_3O_4$	−127.21	[30]
$3MnO + 0.5O_2 = Mn_3O_4$	−58.98	[35]
$3CoO + 0.5O_2 = Co_3O_4$	28.862	This work

principle have to be represented in a three-dimensional plot, where, for example, the vertical axis could represent $\log a_{O_2}$ and the basal plane the Gibbs composition triangle. By projecting phase stability limits for different, constant oxygen activities onto the basal plane one can obtain two-dimensional diagrams containing phase stability information. Such diagrams have been discussed previously [43].

Figure 1 shows the site preference energies of the individual ions that have been chosen to fit the phase equilibria in all systems in comparison with site preference energies reported previously in the literature. After testing a large number of combinations of site preference energies, we decided that the best results were obtained with the values given by Pelton *et al.* [16], and also chose the redox energies ΔG^{ij}_{red} given by these authors. In the following, the phase equilibria results for the three quasi-binary subsystems of the Co–Fe–Mn–O systems are presented first. Then, the results for the quasi-ternary system are discussed. In all cases, the resulting cation distributions in the spinel solid solutions are also shown and are compared with conclusions based on other experimental data.

5.1. *The* Fe–Co–O *system*

Figure 2 shows experimental data for the stability limits of the spinel and rock-salt structure phases at 1200°C from different investigations [36, 37, 44]. The solid lines limiting the two-phase region have been calculated in [29]. The stability of the spinel solid solution decreases abruptly for values of $x > 0.33$. The dashed and dashed–dotted lines limiting the two-phase region have been obtained in this study by modelling. The site preference energies used for this fit are shown in Fig. 1 and are the same as reported in [16] as were the redox energies. The change of the free energy of the rock-salt structure phase with oxygen activity has been taken into account by an exact treatment of the nonstoichiometry of the oxide solid solution [29] as discussed before. To obtain a

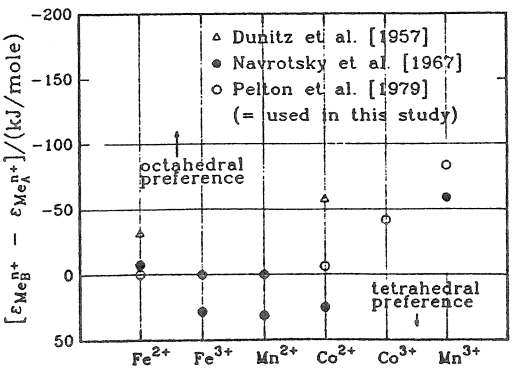

Fig. 1. Single ion site preference energies in spinel phases.

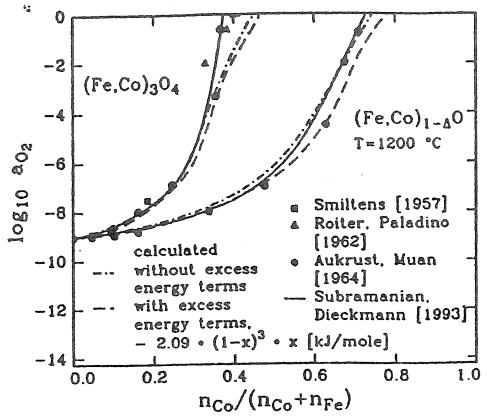

Fig. 2. Spinel and rock-salt structure phase stability limits at 1200°C for the Co–Fe–O system.

more precise fit, it was necessary to use one binary excess energy term in the spinel solid solution. This excess energy was $-2.09 \cdot x^3 \cdot y$ kJ/mol in the abbreviated notation of eqn (38). The effect of the inclusion of this excess energy term on the phase equilibria is demonstrated in Fig. 2. The influence of this term on the results obtained for the cation distribution is shown in Figs 3a and b. It is worth noting that the influence on the cation distribution is negligible, while it is small for the phase equilibria. The redox and exchange reactions between different ions on the tetrahedral and octahedral sites are the principal controlling reactions for the cation distribution in the solid solution. Hence, the cation distribution is not significantly affected by the excess energy terms in the spinel phase. It may be noted that at $x = 0.4$ (the highest value of x in Fig. 2 for the spinel phase), this term amounts to less than 0.1 kJ. Overall, the fit obtained for the phase stability limits is acceptable. However a few discrepancies exist. A possible reason for these could be the exclusion of the nonstoichiometry of the spinel solid solution. For pure Fe_3O_4 a random cation distribution has been assumed at 1200°C, and hence the exchange reaction ΔG^{ex}_{FeFe} has a value of 0 kJ/mol. This distribution has also been deduced from experimental studies of the thermopower and electrical conductivity of magnetite [45, 46]. Co_3O_4 is not stable at 1200°C at one atm total pressure. Hence its cation distribution is debatable. A recent high temperature X-ray diffraction study suggests that the distribution tends towards a disordered normal spinel [47]. A value of 25.1 kJ/mol [16] for the exchange reaction ΔG^{ex}_{CoCo} results in a distribution slightly deviating from normal at 1200°C.

Due to the abrupt decrease in the stability of the spinel region for cobalt mole fractions greater than 0.33 at a temperature of 1200°C, most investigations have been made at lower cobalt contents. Cation

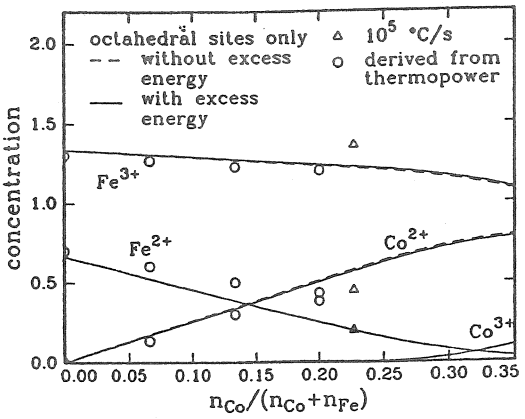

(a)

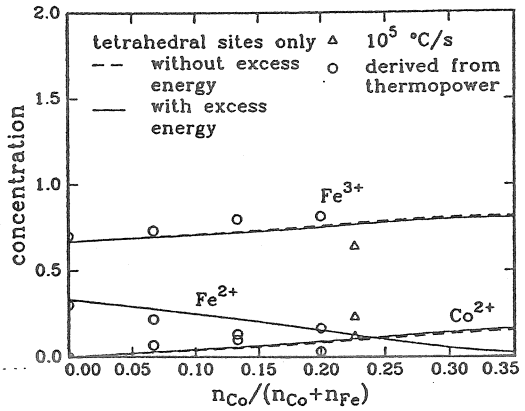

(b)

Fig. 3. Effect of the introduction of an excess energy term for the solid solution $(Co_xFe_y)_3O_4 (x + y = 1)$ at 1200°C on the cation distribution on (a) octahedral sites; and (b) tetrahedral sites: – – – without regular excess energy terms, and —— with the regular excess energy term $-2.09 \cdot y^3 \cdot x$ kJ/mol. The individual data points shown stem from thermopower data from [48]; the data on samples quenched with a rate of 10^5°C/s are from [50].

distribution data for the Fe_3O_4–Co_3O_4 solid solution are available in the literature. They have been derived from thermopower data [48] measured at high temperatures. Unfortunately, several assumptions are involved in the interpretation of such thermopower data. Some of these assumptions are: (i) Co^{3+} ions are absent at $x < 0.33$; (ii) a small polaron conduction is operative and involves only Fe ions on octahedral sites; and (iii) the entropy contribution from the heat of transport of the electrons between the sites can be neglected. Despite the uncertainties introduced by these assumptions, trends of the data sets derived from the experimental studies and from calculations performed in our study are in reasonable agreement (see Figs 3a,b). Samples which have been quenched from high temperatures to freeze in the high-temperature cation distributions were analyzed by Mössbauer spectroscopy and magnetization techniques [49, 50]. The results of these investigations show that the relaxation time for the cation rearrangement between the sites is very short in comparison to quenching rates of 10^5°C/s above 900°C [49]. The concentrations of the different ions in the tetrahedral and octahedral sites in samples of $(Co_{0.233}Fe_{0.767})_3O_4$ quenched from 1200°C at a rate of 10^5°C/s [50] are displayed in Figs 3a,b. The concentrations are in reasonable agreement with the values calculated in this study.

5.2. *The* Fe–Mn–O *system*

As seen in Fig. 4, agreement between the phase equilibria obtained in this study and those calculated in [28] is satisfactory. An excess energy term in the spinel phase was required. This excess energy term was $-6.28 \cdot (1 - x - y) \cdot y^3$ kJ/mol (in the abbreviated notation of eqn (38)). The effect of this excess energy term on the phase equilibria is shown in Fig. 4 and on the cation distribution in the solid solution of Figs 5a,b.

For the cation distribution, several investigations have been performed. Disagreement exists for the charge of the valence states in the spinel structure for the pure oxide Mn_3O_4. The presence of Mn^{2+} and Mn^{3+} [51], Mn^{2+} and Mn^{4+} [5, 52] and combinations of the three valence states [53, 54] have been proposed. Here, a nearly normal distribution is assumed with the presence of Mn^{2+} and Mn^{3+} ions only. This is modelled by a value of 83.6 kJ/mol for the exchange reaction, ΔG^{ex}_{MnMn} [16]. Fe_3O_4 is assumed random with $\Delta G^{ex}_{FeFe} = 0$. With the selection of these values and the exchange and redox reactions between the ions, one can calculate the cation distribution across the solid solution. The trends of the cation distribution in the binary solid solution can be compared with the data available in the literature. The distribution of the various charged cations has been discussed in detail [54] by attempting to interpret

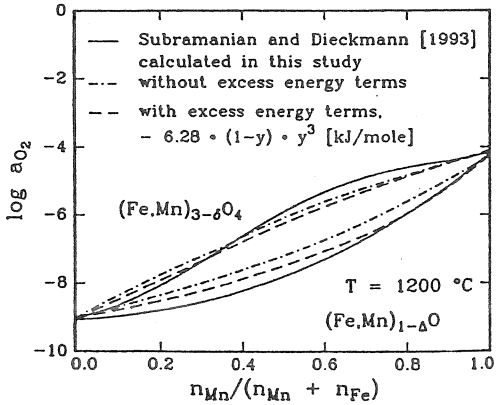

Fig. 4. Two-phase region between spinel and rock-salt structure phases in the Fe–Mn–O system at 1200°C.

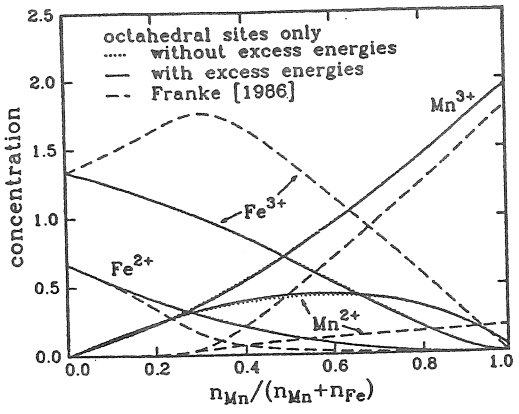

(a)

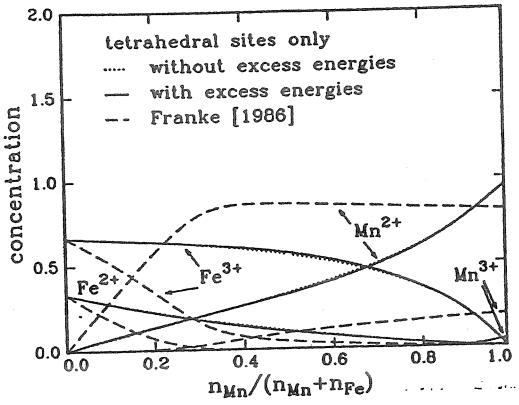

(b)

Fig. 5. Effect of the introduction of an excess energy term in the Fe–Mn–O system at 1200°C on the cation distribution on (a) octahedral sites; and (b) tetrahedral sites: ···· calculated without regular excess energy terms, —— calculated with the regular excess energy term $-6.28 \cdot y^3 \cdot (1-y)$ kJ/mol, and – – – calculated in [55].

simultaneously results from thermopower, conductivity and Mössbauer studies. However, it is worth noting that the Mössbauer studies were performed on quenched samples and that assumptions were made in the analysis of electrical conductivity and thermopower data. Since the assumption of a disproportionation reaction, leading to the presence of all three valence states, Mn^{2+}, Mn^{3+} and Mn^{4+}, in the spinel structure was introduced, the data from [54] cannot be compared with our present modelling. Another detailed modelling of the cation distribution in Fe_3O_4–Mn_3O_4 at 1200°C has been made by taking into account only 2+ and 3+ charged ions and their reactions with the point defects present in the spinel. The underlying assumption was a constant defect formation energy at all compositions in the solid solution [55]. The concentrations of the different ions in the tetrahedral and octahedral sites obtained from [55] are compared with the values from this study in Figs 5a,b. The concentrations and trends obtained are considerably different. To obtain a clearer picture of the cation distribution, experimental *in-situ* investigations which provide direct structural information are needed.

5.3. *The* Co–Mn–O *system*

Experimental data for the two-phase region between the spinel and rock-salt structure phases at 1200°C [42] are shown in Fig. 6. The effect of the nonstoichiometry of $Mn_{1-\Delta}O$ on the rock-salt structure solid solution was taken into account by using a simple approximation as explained before. The nonstoichiometry data in $Mn_{1-\Delta}O$ can be extrapolated reliably up to a value of $\log a_{O_2} = -2$. Hence, the calculation of the phase diagram is possible only up to $\log a_{O_2} = -2$. The stability limits extrapolated to higher oxygen activities are shown as dashed lines in the figure. With the site preference energies and redox equilibria fixed for the two other systems, under the constraints of the model, the values for this system, Co–Mn–O, cannot be changed without changing the values for the systems Co–Fe–O and/or Fe–Mn–O. Using the values from these systems, the phase equilibria in Fig. 6 have been calculated. Nonstoichiometry was neglected in the spinel phase and no regular solution excess energy terms were used in the spinel phase. Since the site preference energies are the same as reported in [16], and no excess energy terms have been used, the cation distribution obtained is identical to that calculated in [16].

5.4. *The* Co–Fe–Mn–O *system*

For this quasi-ternary system, the stability limits of the spinel and rock-salt structure phases at different oxygen activities at constant temperature and total pressure are represented as projections onto the Gibbs composition triangle. Experimental data for

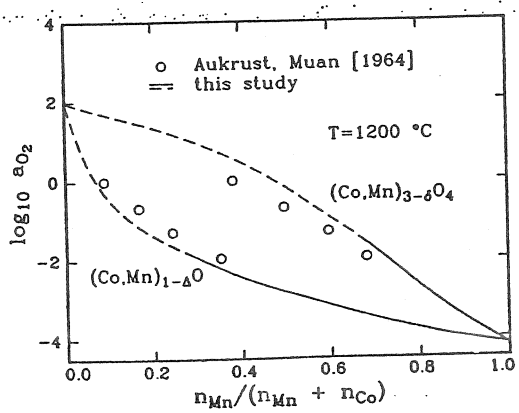

Fig. 6. Two-phase region between spinel and rock-salt structure phases in the Co–Mn–O system at 1200°C.

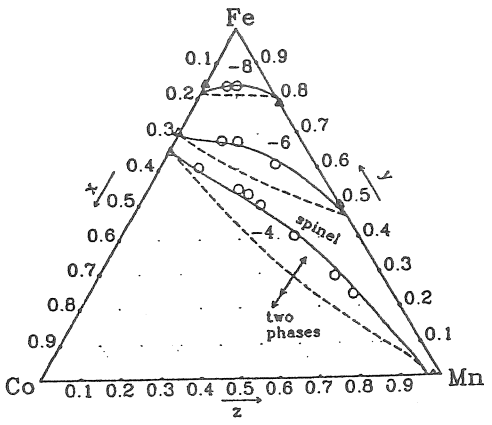

(a)

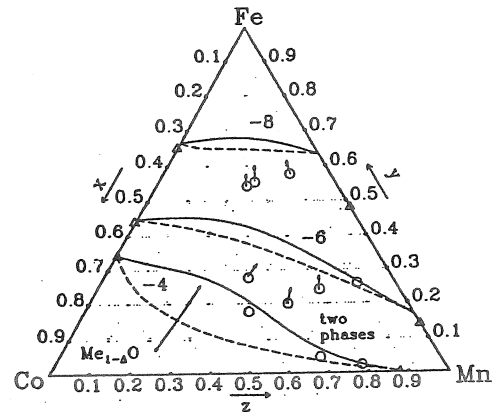

(b)

Fig. 7. Stability limits of oxide solid solutions in the Co–Fe–Mn–O system at 1200°C. (a) Stability limit of the spinel phase towards the rock-salt structure phase; and (b) stability limit of the rock-salt structure phase towards the spinel phase: —— calculated with the excess energy term $+16.74 \cdot x \cdot y \cdot (1-x-y)$ kJ/mol, and --- calculated without excess energy terms. Experimental points: △ from [28], [29] and [42], ○ from [43].

the lower stability limit of the spinel phase towards the rock-salt structure phase [43] are shown in Fig. 7a. In Fig. 7b, experimental data for the stability limit of the rock-salt structure phase towards the spinel phase are displayed. As explained earlier, the experimental data for the quasi-binary phases were fitted by using a set of site preference and redox energies. The same set of values has also been used in the calculation of phase equilibria between the spinel and rock-salt structure phases in the quasi-ternary system. The stability limits of the spinel and rock-salt structure phases were calculated by free energy minimization for specific oxygen activities and then projected onto the basal plane. The dashed lines shown in Figs 7a and b have been obtained without using ternary excess energies. The introduction of an excess energy term for the spinel solid solution of the form of eqn (39) with $a = 16.74 \cdot x \cdot y \cdot (1-x-y)$ kJ/mol (in the abridged notation) leads to a significant improvement of the fit, especially for the lower stability limit of the spinel structure. The solid lines in Fig. 7a have been obtained in this way. The fit for the upper stability limit of the rock-salt structure phase improves at an oxygen activity of 10^{-4}, but deteriorates at lower oxygen activities. It is worth noting that the excess energy introduced at the median of the composition triangle has a maximum value of only 0.6 kJ. Presently, no explanation can be offered for its origin, its magnitude and the form chosen.

The experimental data presented in Fig. 7b are slightly different from those previously reported [43] for the Fe–Mn–O system. The reason is that the data shown in [43] were only estimated while the new data points were taken from the recent study of the two-phase region in the Fe–Mn–O system at 1200°C [28]. The agreement obtained with the experimental data at all oxygen activities for the lower stability limit of the spinel phase is good. Agreement is not as good for the upper stability limit of the rock-salt structure phase. This could be due to the difficulty in experimentally detecting this stability limit (for details see [43]) and/or due to the approximations used for modelling the nonstoichiometry of $(Co, Fe, Mn)_{1-\Delta}O$ as a function of oxygen activity.

Figure 8 shows the projection of phase stability limits at a constant oxygen activity of 10^{-4} at 1200°C. The two-phase region where the spinel and rock-salt structure phases coexist is enclosed between two solid lines. These lines have been calculated by using a ternary excess energy term in the spinel phase. The calculations performed allow also the determination

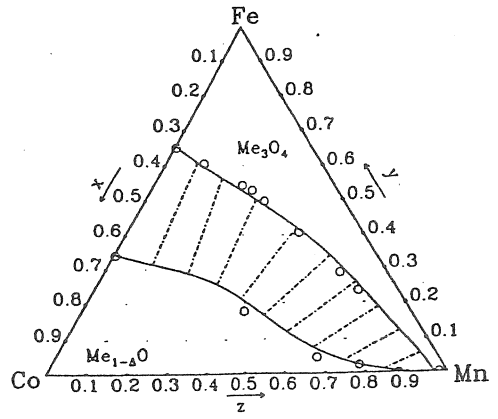

Fig 8. Two-phase region between spinel and rock-salt structure phases in the Co–Fe–Mn–O system at 1200°C and $\log a_{O_2} = -4$. Tie-lines show compositions of coexisting spinel and rock-salt structure phases: —— calculated with the excess energy term $+16.736 \cdot x \cdot y \cdot (1-x-y)$ kJ/mol. Experimental points: ○ from [29], [42] and [43].

of the compositions of coexisting spinel and rock-salt structure phases. The tie lines shown in Fig. 8 are an example of results obtained from such a calculation. Diagrams similar to Fig. 8 can be obtained for other oxygen activities.

Figure 9 shows an example for cation distribution information available from the modelling performed. In this figure, calculated concentrations of the different ions on octahedrally and tetrahedrally coordinated cation lattice sites are displayed for the ternary solid solution $(Co_{0.2}Fe_yMn_{0.8-y})_3O_4$ at 1200°C.

Overall, it can be stated that a successful extension of the modelling of quasi-binary phases has been made to quasi-ternary phases on the basis of the sub-lattice model. A good agreement between experimental and calculated data for the lower stability limit of the spinel phase has been obtained. However, some problems still exist for the upper stability limit of the rock-salt structure phase.

The cation distributions resulting from the present modelling give a semi-quantitative idea of the concentrations of the different ions in octahedral and tetrahedral lattice sites. In the Co_3O_4–Fe_3O_4–Mn_3O_4 spinel solid solution this modelling provides information about the general trends of the distribution of the 6 different ions on two types of lattice sites. Some experimental information about the cation distribution is available for the high iron content region. However, this has been deduced from thermopower and conductivity data by using different, partly unproven, assumptions [56]. Nevertheless, the trends shown in Figs 10a and b are in reasonable agreement with the values derived in [56]. The effect of the ternary excess energy term on the cation distribution is negligible, as in the case of the quasi-binary phases.

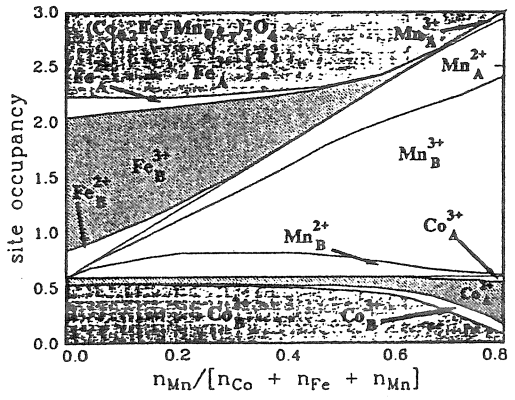

Fig. 9. Cation distribution in $(Co_{0.2}Fe_yMn_{0.8-y})_3O_4$ at 1200°C. The spacing between two consecutive lines for any given manganese content gives the concentration of the ions in the region enclosed by these two lines.

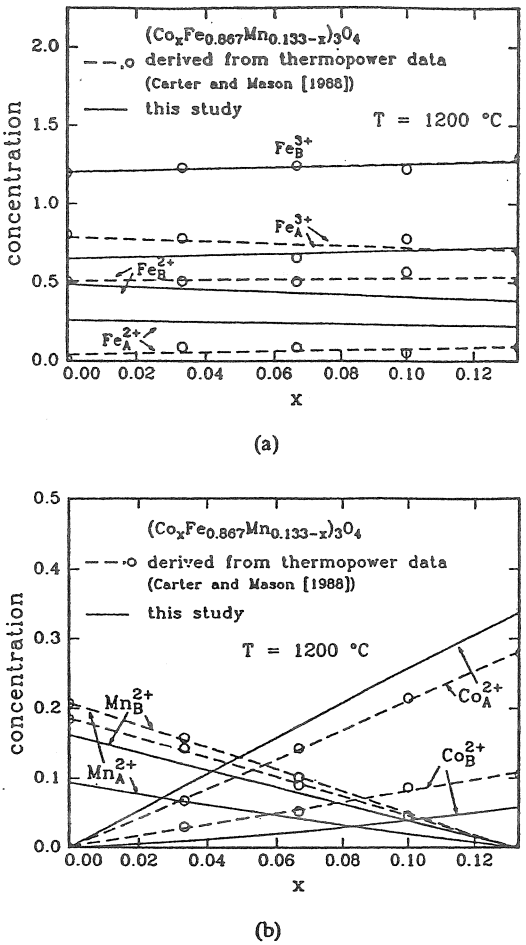

Fig. 10. Comparison between cation distribution data derived from thermopower studies [56] and calculated in this study for $(Co_xFe_{0.867}Mn_{0.133-x})_3O_4$ at 1200°C: (a) iron ions only; and (b) cobalt and manganese ions.

6. CONCLUSIONS

A sub-lattice model has been used to model the spinel structure phase in the Co–Fe–Mn–O system at 1200°C. It is based on the distribution of cations between tetrahedral and octahedral sites. An exact treatment of the nonstoichiometry of the solid solutions of $(Fe, Co)_{1-\Delta}O$ and $(Fe, Mn)_{1-\Delta}O$ has been incorporated into the modelling. A set of spinel site preference energies and redox energies was selected for fitting experimental data for the two-phase region between the spinel and rock-salt structure phases of the quasi-binary boundary systems. These energies were then used to model phase stability limits in the Co–Fe–Mn–O system at 1200°C. The results obtained have been represented as projections of phase stability limits for different oxygen activities onto the Gibbs composition triangle. Cation distributions have been derived for the quasi-binary boundary spinel solid solutions, $(Co, Fe)_3O_4$,

$(Co, Mn)_3O_4$ and $(Fe, Mn)_3O_4$, as well as for the Co_3O_4–Mn_4O_4–Fe_3O_4 solid solution.

Acknowledgements—The authors wish to acknowledge the U.S. Department of Energy for support of this work under Grant DE-FG02-88-ER45357. (This support does not constitute an endorsement by DOE of the views expressed in this article.) Furthermore, they thank the Cornell Ceramics Program for supporting their work. The authors also thank the Cornell Materials Science Center (supported by the National Science Foundation under award No. DMR-9121654) for the use of its facilities. Support from the Natural Sciences and Engineering Research Council of Canada is also gratefully acknowledged.

REFERENCES

1. Hill R. J., Craig J. R. and Gibbs G. V., *Phys. Chem. Miner.* **4**, 317 (1979).
2. Blasse G., *Philips Res. Repts. Suppl.* **3**, 1 (1964).
3. Verwey E. J. W. and De Boer J. H., *J. Chem. Phys.* **16**, 1091 (1948).
4. Schmalzried H., *Z. Physik. Chem. NF* **28**, 203 (1961).
5. Dunitz J. D. and Orgel L. E., *J. Phys. Chem. Solids* **3**, 318 (1957).
6. McClure D. S., *J. Phys. Chem. Solids* **3**, 311 (1957).
7. Navrotsky A. and Kleppa O. J., *J. Inorg. Nucl. Chem.* **29**, 2701 (1967).
8. Navrotsky A., *J. Inorg. Nucl. Chem.* **31**, 59 (1969).
9. O'Neill H. S. C. and Navrotsky A., *Am. Miner.* **68**, 181 (1983).
10. O'Neill H. S. C. and Navrotsky A., *Am. Miner.* **69**, 733 (1984).
11. Cormack A. N., Lewis G. V., Parker S. C. and Catlow C. R. A., *J. Phys. Chem. Solids* **49**(1), 53 (1988).
12. Nell J., Wood B. J. and Mason T. O., *Am. Miner.* **74**, 339 (1989).
13. Nell J. and Wood B. J., *Am. Miner.* **74**, 1000 (1989).
14. Nell J. and Wood B. J., *Am. Miner.* **76**, 405 (1991).
15. Thompson P. and Grimes N. W., *Phil. Mag.* **36**(3), 501 (1977).
16. Pelton A. D., Schmalzried H. and Sticher J., *Ber. Bunsenges. Phys. Chem.* **83**, 241 (1979).
17. Blander M. and Yosim S. J., *J. Chem. Phys.* **39**(10), 2610 (1963).
18. Pelton A. D., *Calphad* **12**(2), 127 (1988).
19. Hillert M. and Staffansson L. I., *Acta. Chem. Scand.* **24**, 3618 (1970).
20. Sundman B. and Argen J., *J. Phys. Chem. Solids* **42**, 297 (1981).
21. Keller M. and Dieckmann R., *Ber. Bunsenges. Phys. Chem.* **89**(10), 1095 (1985).
22. Dieckmann R., *Ber. Bunsenges. Phys. Chem.* **86**(2), 112 (1982).
23. Lu F.-H. and Dieckmann R., *Ceram. Trans* **24**, 185 (1991).
24. Darken L. S. and Gurry R. W., *J. Am. Chem. Soc.* **67**, 1398 (1945).
25. Keller M. and Dieckmann R., *Ber. Bunsenges. Phys. Chem.* **89**(10), 883 (1985).
26. Dieckmann R., *Z. Phys. Chem. NF* **107**, 189 (1977).
27. Aggarwal S. and Dieckmann R., *Ceram. Trans.* **24**, 23 (1991).
28. Subramanian R. and Dieckmann R., *J. Phys. Chem. Solids* **54**(9), 991 (1993).
29. Subramanian R. and Dieckmann R., *J. Phys. Chem. Solids* **55**, 59 (1994).
30. Franke P. and Dieckmann R., *J. Phys. Chem. Solids* **51**(1), 49 (1990).
31. Subramanian R., Tinkler S. and Dieckmann R., *J. Phys. Chem. Solids* **55**, 69 (1994).
32. Kohler F., *Mh. Chem.* **91**, 738 (1960).
33. Eriksson G., *Acta Chem. Scand.* **25**, 2651 (1971).
34. Eriksson G., *Chemica Scripta* **8**, 100 (1975).
35. Keller M., Xue J. and Dieckmann R., *J. Electrochem. Soc.* **138**(11), 3398 (1991).
36. Coughlin J. P., *U.S. Bur. Mines. Bull.* **542**, 19 (1954).
37. Roiter B. D. and Paladino A. E., *J. Am. Ceram. Soc.* **45**, 128 (1962).
38. Aukrust E. and Muan A., *Trans. Met. Soc. AIME*, **230**, 1395 (1964).
39. Budgen W. G. and Pratt J. N., *Trans. Instn. Mining. Metallurgy, Sect. C* **79**, C221 (1970).
40. Enoki E., Hagiwara S., Kaneko H. and Saito Y., *Nippon Kinzoku Gakkhaishi* **41**, 505 (1977).
41. Persels K. L., Ph.D. thesis, Northwestern University (1990).
42. Aukrust E. and Muan A., *Trans. Met. Soc. AIME* **227**, 1195 (1963).
43. Subramanian R. and Dieckmann R., *J. Am. Ceram. Soc.* **75**(2), 120 (1992).
44. Smiltens J., *J. Am. Chem. Soc.* **79**, 4881 (1957).
45. Wu C. C. and Mason T. O., *J. Am. Ceram. Soc.* **64**(9), 520 (1981).
46. Dieckmann R., Witt C. A. and Mason T. O., *Ber. Bunsenges. Phys. Chem.* **87**(6), 495 (1983).
47. Liu X. and Prewitt C. T., *Phys. Chem. Miner.* **17**, 168 (1990).
48. Erickson D. S. and Mason T. O., *J. Solid State Chem.* **59**, 42 (1985).
49. De Guire M. R., O'Handley R. C. and Kalonji G., *J. appl. Phys.* **65**(8) (1989).
50. De Guire M. R., O'Handley R. C. and Kalonji G., *J. Am. Ceram. Soc.* **73**(10), 3002 (1990).
51. Romeijn F. C., *Philips Res. Rep.* **8**, 304 (1953).
52. O'Keeffe M., *J. Phys. Chem. Solids* **21**, 172 (1961).
53. Dorris S. E. and Mason T. O., *J. Am. Ceram. Soc.* **71**(5), 379 (1988).
54. Dorris S. E., Ph.D. thesis, Northwestern University (1986).
55. Franke P., Doctoral thesis, University of Hannover (Federal Republic of Germany) (1987).
56. Carter D. C. and Mason T. O., *J. Am. Ceram. Soc.* 71(4), 213 (1988).